2012

Cosmological Implications of a Stellar Initial Mass Function that Varies with the Jeans Mass in Galaxies

Desika Narayanan
Haverford College, dnarayan@haverford.edu

Monthly Notices
of the
ROYAL ASTRONOMICAL SOCIETY

Mon. Not. R. Astron. Soc. **423,** 3601–3615 (2012) doi:10.1111/j.1365-2966.2012.21159.x

Cosmological implications of a stellar initial mass function that varies with the Jeans mass in galaxies

Desika Narayanan★† and Romeel Davé

Steward Observatory, University of Arizona, 933 N Cherry Ave, Tucson, AZ 85721, USA

Accepted 2012 April 21. Received 2012 April 19; in original form 2012 February 29

ABSTRACT

Observations of star-forming galaxies at high z have suggested discrepancies in the inferred star formation rates (SFRs) either between data and models or between complementary measures of the SFR. These putative discrepancies could all be alleviated if the stellar initial mass function (IMF) is systematically weighted towards more high-mass star formation in rapidly star-forming galaxies. Here, we explore how the IMF might vary under the central assumption that the turnover mass in the IMF, $\hat{M}_{\rm c}$, scales with the Jeans mass in giant molecular clouds (GMCs), $\hat{M}_{\rm J}$. We employ hydrodynamic simulations of galaxies coupled with radiative transfer models to predict how the typical GMC Jeans mass, and hence the IMF, varies with galaxy properties. We then study the impact of such an IMF on the star formation law, the SFR–M_* relation, sub-millimetre galaxies (SMGs) and the cosmic SFR density. Our main results are: the H_2 mass-weighted Jeans mass in a galaxy scales well with the SFR when the SFR is greater than a few $M_\odot$ yr^{-1}. Stellar population synthesis modelling shows that this results in a non-linear relation between SFR and $L_{\rm bol}$, such that SFR $\propto {L_{\rm bol}}^{0.88}$. Using this model relation, the inferred SFR of local ultraluminous infrared galaxies decreases by a factor of $\sim$2, and that of high-z SMGs decreases by a factor of $\sim$3–5. At $z \sim 2$, this results in a lowered normalization of the SFR–M_* relation in better agreement with models, a reduced discrepancy between the observed cosmic SFR density and stellar mass density evolution, and SMG SFRs that are easier to accommodate in current hierarchical structure formation models. It further results in a Kennicutt–Schmidt star formation law with a slope of $\sim$1.6 when utilizing a physically motivated form for the CO–H_2 conversion factor that varies with galaxy physical property. While each of the discrepancies considered here could be alleviated without appealing to a varying IMF, the modest variation implied by assuming $\hat{M}_{\rm c} \propto \hat{M}_{\rm J}$ is a plausible solution that simultaneously addresses numerous thorny issues regarding the SFRs of high-z galaxies.

Key words: stars: formation – stars: luminosity function, mass function – galaxies: formation – galaxies: high-redshift – galaxies: ISM – cosmology: theory.

1 INTRODUCTION

The buildup of stellar mass over cosmic time is a central issue in understanding the formation and evolution of galaxies. A common approach to quantifying stellar growth is to measure the evolution of the star formation rates (SFRs) of galaxies. This is done using a wide variety of tracers from the ultraviolet (UV) to the radio. Generally, all such measures trace the formation rate of higher-mass (typically O and B) stars, while the bulk of the stellar mass forming in lower-mass stars is not directly detected. Hence measuring the true rate of stellar growth requires assuming a conversion between the particular tracer flux and the total stellar mass being generated (e.g. Kennicutt 1998a; Kennicutt & Evans 2012). This requires assuming some stellar initial mass function (IMF), namely the number of stars being formed as a function of mass.

On global cosmological scales, multi-wavelength observations of galaxies are converging on a broad scenario for the cosmic SFR evolution (Madau et al. 1996). Galaxies at high redshift appear to be more gas-rich and forming stars more rapidly at a given stellar mass than present-day galaxies (see the recent review by Shapley 2011). The cosmic SFR density rises slowly from early epochs to peak between redshifts $z \approx 1$ and 3, and then declines towards $z = 0$ (e.g.

★E-mail: dnarayanan@as.arizona.edu
†Bart J Bok Fellow.

Hopkins & Beacom 2006). This global evolution is also reflected in measurements of the SFRs of individual galaxies, which grow significantly at a given stellar mass from today out to $z \sim 2$, prior to which they show a much slower evolution (e.g. Daddi et al. 2005; Davé 2008; González et al. 2010; Hopkins et al. 2010).

Meanwhile, recent advances in near-infrared capabilities have enabled measurements of the buildup of stellar mass out to high redshifts, as traced by more long-lived stars (typically red giants). Nominally, the integral of the cosmic SFR, when corrected for stellar evolution processes, should yield the present-day cosmic stellar mass. Analogously, the time differential of the stellar mass evolution should be the same as measured SFR. Thus in principle there is now a cross-check on the rate of high-mass stars forming relative to lower-mass stars.

Preliminary comparisons along these lines have yielded general agreement out to $z \sim 1$ (e.g. Bell et al. 2007). However, moving to higher redshifts into the peak epoch of cosmic star formation, there are growing hints of discrepancies: the integrated cosmic SFR density seems to exceed the observed stellar mass function (accounting for stellar mass loss; Hopkins & Beacom 2006; Elsner, Feulner & Hopp 2008; Pérez-González et al. 2008; Wilkins, Trentham & Hopkins 2008). These discrepancies are relatively mild, at the factor of 2 to 3 level, so could perhaps be resolved by a more careful consideration of systematic uncertainties in SFR and M_* measures. Indeed, some analyses fail to show strong discrepancies (e.g. Sobral et al. 2012). Nevertheless, it is interesting that when discrepancies are seen, they unanimously favour the idea that the observed stellar mass growth appears slower than expected from the observed SFR.

Theoretical models have made a number of advances towards understanding the observed properties of star-forming galaxies at high redshifts. Simulations advocate a picture in which continual gas accretion from the intergalactic medium (IGM) feeds galaxies with fresh fuel (e.g. Mo, Mao & White 1998; Robertson et al. 2004; Governato et al. 2009; Ceverino, Dekel & Bournaud 2010a; Agertz, Teyssier & Moore 2011) and ultimately drives star formation (Kereš et al. 2005, 2009; Dekel et al. 2009a,b). In such models, stars typically form at rates proportional to the global gas accretion rate from the IGM, regulated by feedback processes (Springel & Hernquist 2003; Davé, Oppenheimer & Finlator 2011). Such a scenario predicts a fairly tight and nearly linear relation between SFR and stellar mass for star-forming galaxies (e.g. Davé et al. 2000; Finlator et al. 2006). Observations have now identified and quantified such a relation out to $z \sim 6$–8 (Daddi et al. 2007; Noeske et al. 2007a,b; Stark et al. 2009; McLure et al. 2011), which has come to be called the 'main sequence' of galaxy formation. The bulk of cosmic star formation appears to occur in galaxies along this main sequence, while merger-driven starbursts contribute $\lesssim$20 per cent globally (e.g. Rodighiero et al. 2011; Wuyts et al. 2011).

Although this scenario broadly agrees with observations, a small but persistent discrepancy has been recently highlighted between the evolution of the main sequence in simulations and observations, particularly during the peak epoch of cosmic star formation ($1 \lesssim z \lesssim 3$). In it, the rate of stellar mass growth at these redshifts in models is typically smaller by $\sim$2–3$\times$ than the observed SFRs. This discrepancy exists for both cosmological hydrodynamic simulations (Davé 2008) and semi-analytic models (SAMs; Daddi et al. 2007; Elbaz et al. 2007), and is to the first order independent of model assumptions about feedback (Davé 2008). This is further seen both in the global cosmic SFR (Wilkins et al. 2008) and when comparing individual galaxies at a given M_* (Davé 2008). Similarly, galaxy formation simulations that utilize a variety of methods all show a paucity of galaxies that form stars as rapidly as galaxies with the highest SFRs at $z \sim 2$, the sub-millimetre galaxies (SMGs) (Baugh et al. 2005; Davé et al. 2010; Hayward et al. 2011). In all cases, the models tend to favour lower true SFRs than implied by using available tracers and using conversion factors based on a canonical IMF.

One possible but speculative solution to all these discrepancies is that the stellar IMF in galaxies at $z \sim 2$ is different from what is measured directly in the Galaxy (e.g. Kang et al. 2010). The discrepancies described above, between the various observations as well as between models and data, would all be mitigated by an IMF that forms somewhat more high-mass stars than low-mass ones at those epochs compared to the present-day IMF.[1] Nevertheless, it is important to point out that at present there is no firm evidence that the IMF varies strongly from the locally observed one (see the review by Bastian, Covey & Meyer 2010). Locally, some observations suggest that a top-heavy/bottom-light IMF may apply to the Galactic Centre (Nayakshin & Sunyaev 2005; Stolte et al. 2005). Similarly, Rieke et al. (1993) and Förster Schreiber et al. (2003) suggest a turnover mass a factor of $\sim$2–6 larger than in a traditional (Kroupa 2002) IMF in the nearby starburst galaxy M82. Simultaneous fits to the observed cosmic SFR density, integrated stellar mass measurements and cosmic background radiation favour a 'paunchy' IMF that produces more stars at intermediate masses (Fardal et al. 2007). van Dokkum (2008) suggested that the IMF may be more top-heavy at high redshift ($z \approx 0.8$) based on an analysis of the evolution of the colours and mass-to-light ratios of early-type galaxies. However, these observations can all be interpreted without the need for IMF variations (Bastian et al. 2010). Beyond this, some observations find evidence for a *bottom-heavy* IMF in $z = 0$ early-type galaxies (van Dokkum & Conroy 2011; Cappellari et al. 2012; Conroy & van Dokkum 2012). It is therefore interesting to examine whether an IMF-based solution is viable and consistent with a broad suite of observations, both locally and in the distant Universe.

In this paper, we explore the cosmological consequences of a *physically based* model for IMF variations. Past work has generally focused on *empirically* determining the amount of IMF variation needed in order to solve one (or more) of the above problems (e.g. Fardal et al. 2007; Davé 2008; van Dokkum 2008; Wilkins et al. 2008). Here, instead, we make a single critical assumption, first forwarded by Jeans, and later expanded upon by Larson (2005) and Tumlinson (2007): *the IMF critical mass ($\hat{M}_c$) scales with the Jeans mass in a giant molecular cloud* (GMC). For reference, we call this the Jeans mass conjecture. We employ hydrodynamic simulations of isolated galaxies and mergers including a fully radiative model for the interstellar medium (ISM) to predict the typical Jeans mass of GMCs in galaxies with different physical conditions, corresponding to quiescent and starbursting systems both today and at $z = 2$. Applying the Jeans mass conjecture, we then make a prediction for how the IMF varies with global galaxy properties, and explore the implications for such variations on the discrepancies noted above.

We emphasize that the main purpose of this paper is to utilize numerical models of the molecular ISM in galaxies to investigate the consequences of an IMF in which $\hat{M}_c$ scales with M_J. We do not directly argue for such a scaling relationship; this is taken as an assumption, and we only seek to study its implications in a

[1] This could be described as a 'top-heavy' IMF, which we specify as an IMF whose high-mass slope is different from local, or a 'bottom-light' IMF, which we define as retaining the same high-mass slope but forming fewer low-mass stars. This paper focuses on bottom-light IMFs.

cosmological context. For the reader's edification, we present arguments both for and against the Jeans mass conjecture in Section 5.

This paper is outlined as follows. In Section 2, we detail our numerical models. In Section 3, we discuss variations of the IMF versus galaxy SFRs. In Section 4, we investigate the effect of this model on derived SFRs, paying particular attention to the star formation law (Sections 4.1 and 4.2), the SFR–M_* relation at high redshift (Section 4.3) and the evolution of the cosmic SFR density (Section 4.5). In Section 5, we present a discussion; and in Section 6, we summarize.

2 NUMERICAL METHODS

Our main goal is to simulate the global physical properties of GMCs in galaxies, and understand the effect of the varying Jeans mass on observed SFRs. These methods and the corresponding equations are described in significant detail in Narayanan et al. (2011b,c); for the sake of brevity, we summarize the relevant aspects of this model here, and refer the interested reader to those papers for further detail.

We first simulate the evolution of galaxies hydrodynamically using the publicly available code GADGET-3 (Springel 2005; Springel, Di Matteo & Hernquist 2005). In order to investigate a variety of physical environments, we consider the evolution of disc galaxies in isolation, major (1:1 and 1:3) mergers and minor (1:10) mergers at both low ($z = 0$) and high ($z = 2$) redshifts. These simulations are summarized in table A1 of Narayanan et al. (2012). The discs are initialized according to the Mo et al. (1998) model, and embedded in a live dark matter halo with a Hernquist (1990) density profile. Galaxy mergers are simply mergers of these discs. The halo concentration and virial radius for a halo of a given mass are motivated by cosmological N-body simulations, and scaled to match the expected redshift evolution following Bullock et al. (2001) and Robertson et al. (2006).

For the purposes of the hydrodynamic calculations, the ISM is modelled as multi-phase, with cold clouds embedded in a hotter phase (McKee & Ostriker 1977). The phases exchange mass via radiative cooling of the hot phase, and supernova heating of cold gas. Stars form within the cold gas according to a volumetric Kennicutt–Schmidt (KS) star formation relation, SFR $\sim \rho_{\rm cold}^{1.5}$, with normalization set to match the locally observed relation (Kennicutt 1998a; Springel 2000; Cox et al. 2006).

In order to model the physical properties of GMCs within these model galaxies, we perform additional calculations on the smoothed particle hydrodynamics (SPH) models in post-processing. We first project the physical properties of the galaxies on to an adaptive mesh with a 5^3 base, spanning 200 kpc. The cells recursively refine in an oct-subdivision based on the criteria that the relative density variations of metals should be less than 0.1, and the V band optical depth across the cell $\tau_{\rm V} < 1$. The smallest cells in this grid are of the order of ∼70 pc across, just resolving massive GMCs.

The GMCs are modelled as spherical and isothermal. The H_2–H I balance in these cells is calculated by balancing the photodissociation rates of H_2 against the growth rate on dust grains following the methodology of Krumholz, McKee & Tumlinson (2008, 2009a,b). This assumes equilibrium chemistry for the H_2. The GMCs within cells are assumed to be of constant density, and have a minimum surface density of 100 $M_\odot$ pc^{-2}. This value is motivated by the typical surface density of Local Group GMCs (McKee & Ostriker 2007; Bolatto et al. 2008; Fukui & Kawamura 2010), and exists to prevent unphysical conditions in large cells towards the outer regions of the adaptive mesh. In practice, the bulk of the GMCs in galaxies of interest for this study (i.e. galaxies where the galactic environment has a significant impact on the Jeans mass) have surface densities above this fiducial threshold value. With the surface density of the GMC known, the radius (and consequently mean density) is known as well. Following Narayanan et al. (2011b), to account for the turbulent compression of gas, we scale the volumetric densities of the GMCs by a factor $e^{\sigma_\rho^2/2}$, where $\sigma_\rho \approx \ln(1 + M_{\rm 1D}^2/4)$, and $M_{\rm 1D}$ is the one-dimensional Mach number of turbulence (Ostriker, Stone & Gammie 2001; Padoan & Nordlund 2002).

Because this study centres around understanding the Jeans scale in GMCs, the thermal state of the molecular ISM must be known. Following Krumholz, Leroy & McKee (2011) and Narayanan et al. (2011b,c), we consider the temperature of the H_2 gas as a balance between heating by cosmic rays, grain photoelectric effect, cooling by CO or C II line emission, and energy exchange with dust. The cosmic ray flux is assumed to be that of the mean Galactic value.[2] Formally, if we denote heating processes by Γ, cooling by Λ and energy exchange with Ψ, we solve the following equations:

$$\Gamma_{\rm pe} + \Gamma_{\rm CR} - \Lambda_{\rm line} + \Psi_{\rm gd} = 0 \quad (1)$$

$$\Gamma_{\rm dust} - \Lambda_{\rm dust} - \Psi_{\rm gd} = 0. \quad (2)$$

We refer the reader to Krumholz et al. (2011) and Narayanan et al. (2011b) for the equations regarding the photoelectric effect and cosmic ray heating terms.

The dust temperature is calculated via the publicly available dust radiative transfer code SUNRISE (Jonsson 2006; Jonsson, Groves & Cox 2010; Jonsson & Primack 2010). We consider the transfer of both stellar light from clusters of stars and radiation from a central active galactic nucleus (though this plays relatively little role in these simulations). The stars emit a STARBURST99 spectrum (Leitherer et al. 1999; Vázquez & Leitherer 2005), where the metallicity and ages of the stellar clusters are taken from the hydrodynamic simulations. The radiation then traverses the galaxy, being absorbed, scattered and reemitted as it escapes. The evolving dust mass is set by assuming a constant dust-to-metals ratio comparable to the mean Milky Way (MW) value (Dwek 1998; Vladilo 1998; Calura, Pipino & Matteucci 2008), and takes the form of the $R = 3.15$ (Weingartner & Draine 2001) grain model as updated by Draine & Li (2007). The dust and radiation field are assumed to be in equilibrium, and the dust temperatures are calculated iteratively. Energy exchange between gas and dust becomes important typically around $n \sim 10^4$ cm^{-3}. Henceforth, we shall refer to this as the density where grain–gas coupling becomes important.

The gas cools either via C II or CO line emission. The fraction of H_2 where most of the carbon is in the form of CO (versus atomic form) is determined following the SAM of Wolfire, Hollenbach & McKee (2010), which is a metallicity-dependent model (such that at lower metallicities, most of the carbon is in atomic form, and at higher metallicities, it is mostly in the form of CO):

$$f_{\rm CO} = f_{\rm H2} \times e^{-4(0.53-0.045\,\ln\frac{G_0'}{n_{\rm H}/{\rm cm}^{-3}}-0.097\ln Z')/A_{\rm v}}, \quad (3)$$

where G_0' is the UV radiation field with respect to that of the solar neighbourhood, and $A_{\rm V}$ is the visual extinction, $A_{\rm V} = \frac{N_{\rm H}}{1.87\times10^{21}\ {\rm cm}^{-2}} Z'$ (Watson 2011). If $f_{\rm CO} > 0.5$, we assume that the gas

[2] Tests described by Narayanan et al. (2012) show that even under the assumption of a scaling where cosmic ray flux scales with the SFR of a galaxy, the typical thermal profile of H_2 gas in a given galaxy is unchanged. This is because, in these environments, energy exchange with dust tends to dominate the temperature.

cools via CO line emission; else, C II. The line emission is calculated via the publicly available escape probability code as detailed in Krumholz & Thompson (2007).

While the temperature model is indeed somewhat complicated, the typical temperature of a cloud can be thought of in terms of the dominant heating effects at different densities. At low densities ($n \sim$ 10–100 cm^{-3}), the gas cools via line cooling to $\sim$8 K, the characteristic temperature imposed by cosmic ray heating. At high densities ($n \gtrsim 10^4$ cm^{-3}), grain–gas coupling becomes efficient, and the gas rises to the dust temperature. At intermediate densities, the temperature is typically in between 8 K and the dust temperature.

3 THE RELATION BETWEEN JEANS MASS AND STAR FORMATION RATE

We begin by examining the conditions under which the Jeans mass in GMCs in a galaxy may vary. We define the characteristic Jeans mass, $\hat{M}_{\rm J}$, as the H_2 mass-weighted Jeans mass across all GMCs in a galaxy, and consider the deviations of this quantity. The density term in the Jeans mass calculation is the mean density of the GMC. In Fig. 1, the top panel shows the SFR as a function of time for an unperturbed $z = 0$ disc galaxy, a $z = 0$ major 1:1 galaxy merger and a $z = 2$ disc. The second panel shows the evolution of $\hat{M}_{\rm J}/250$ M$_\odot$.

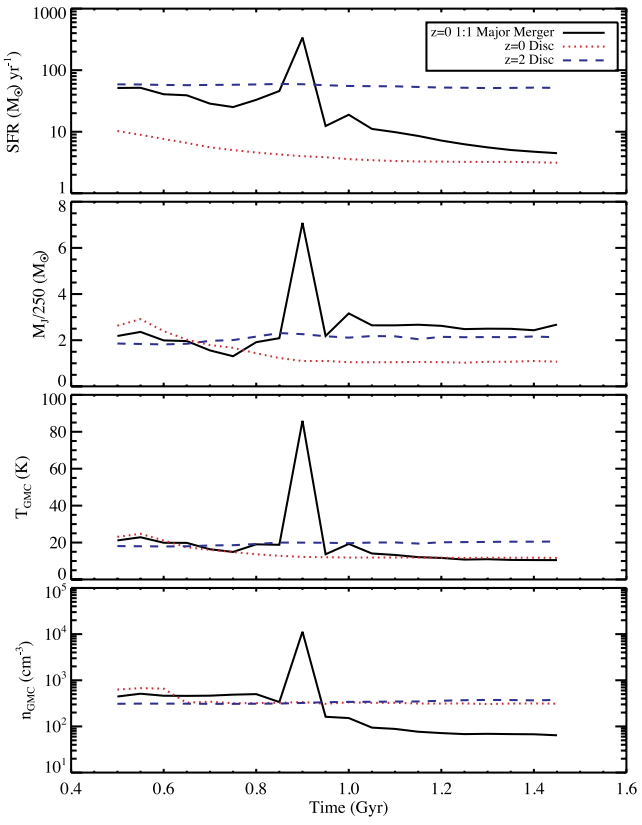

Figure 1. Evolution of SFR, enhancement in $\hat{M}_{\rm J}$ (above 250 M$_\odot$, a typical Jeans mass for an $n = 10^2$ cm^{-3}, $T = 10$ K GMC), H_2 mass-weighted GMC temperature and H_2 mass-weighted GMC density in a model $z = 0$ disc galaxy, $z = 2$ disc galaxy and $z = 0$ 1:1 major galaxy merger. During the merger, warm dust heated by the starburst couples efficiently with the gas and raises the temperature of H_2 molecules. This drives a rise in the typical Jeans mass of GMCs. $z = 0$ quiescent discs, on the other hand, have much more moderate conditions in their ISM. High-z discs represent intermediate cases.

250 M$_\odot$ is the Jeans mass for physical conditions as found in local discs like the MW, namely $n = 1$–2×10^2 cm^{-3} and $T = 10$ K. Our disc galaxy has a baryonic mass of $\sim 5 \times 10^{10}$ M$_\odot$, and is the fiducial MW model in Narayanan et al. (2011b). We note that the fiducial $z = 0$ MW model naturally produces densities, temperatures and $\hat{M}_{\rm J}$ as observed in the MW, thereby providing an important check for our ISM model. The major merger is a merger of two $M_{\rm bar} = 1.5 \times 10^{11}$ M$_\odot$ galaxies. The high-z disc model is an unperturbed $M_{\rm bar} = 10^{11}$M$_\odot$ disc. The remaining panels show the evolution of the characteristic temperatures and the characteristic GMC densities.[3]

For the bulk of the $z = 0$ disc's life, and during non-interacting stages of the galaxy merger, the GMCs are relatively quiescent, retaining surface densities near 100 M$_\odot$ pc^{-2}, and temperatures near the floor established by cosmic ray heating of $\sim$10 K. During the merger-induced starburst, however, the story is notably different. Gas compressions caused by the nuclear inflow of gas during the merger cause the average density to rise above 10^4 cm^{-3} in GMCs. At this density, grain–gas energy exchange becomes quite efficient. At the same time, dust heating by the massive stars formed in the starburst causes the mass-weighted dust temperature to rise from $\sim$30 to $\sim$80 K. Consequently, the kinetic temperature of the gas reaches similar values. While the mean gas density also rises during the merger, the Jeans mass goes as $T^{3/2}/n^{1/2}$. As a result, $\hat{M}_{\rm J}$ rises by a factor of $\sim$5 during the merger-induced starburst. The $z = 2$ disc represents an intermediate case: high gas fractions and densities drive large SFRs, and thus warmer conditions in the molecular ISM.

The characteristic Jeans mass in a galaxy is well parametrized by the SFR. In Fig. 2, we plot the SFRs of all of the galaxies in our simulation sample against their $\hat{M}_{\rm J}$. The points are individual time snapshots from the different galaxy evolution simulations. At high SFRs, dust is warmed by increased radiation field, and thermally couples with the gas in dense regions. The increased temperature drives an increase in the Jeans mass, resulting in roughly a power-law increase of $\hat{M}_{\rm J}$ with SFR.

This relation does not extend to SFR $\lesssim$ 3–5 M$_\odot$ yr^{-1}. Here, the mean densities become low enough ($n < 10^4$ cm^{-3}) that energy exchange with dust no longer keeps the gas warm. Cosmic rays dominate the heating in this regime, and the gas cools to $\sim$8–10 K, the typical temperature that results from the balance of CO line cooling and cosmic ray heating. Because the temperatures are relatively constant, and the characteristic densities of the order of $\sim$10–100 cm^{-3}, the Jeans mass flattens with respect to SFR. There may be additional variations in $\hat{M}_{\rm J}$ at smaller masses, owing e.g. to metallicity variations that we neglect here. For our purposes, we are predominantly interested in higher-z galaxies that generally have SFR $\gg 5$ M$_\odot$ yr^{-1}, so we do not try to characterize in detail the behaviour of $\hat{M}_{\rm J}$ at lower SFR.

The resulting relation is well-fitted by a power law $\hat{M}_{\rm J}/250$ M$_\odot$ $= 0.5 \times$ SFR$^{0.4}$ at SFR $\gtrsim 3$ M$_\odot$ yr^{-1}. This fit is shown in Fig. 2 by the black line, and extends up to $\sim$1000 M$_\odot$ yr^{-1} in our models. The fit excludes the low SFR tail at SFR $<$ 3 M$_\odot$ yr^{-1}. There is substantial scatter around the relation owing to the fact that at a given SFR, there may be a variety of physical conditions. For example, galaxies with SFR ~ 50 M$_\odot$ yr^{-1} may represent merger-induced starbursts with extremely warm nuclear

[3] Note that because $\hat{M}_{\rm J}$ is calculated as the H_2 mass-weighted Jeans mass, one cannot convert from the characteristic temperatures and densities shown in Fig. 1 to $\hat{M}_{\rm J}$.

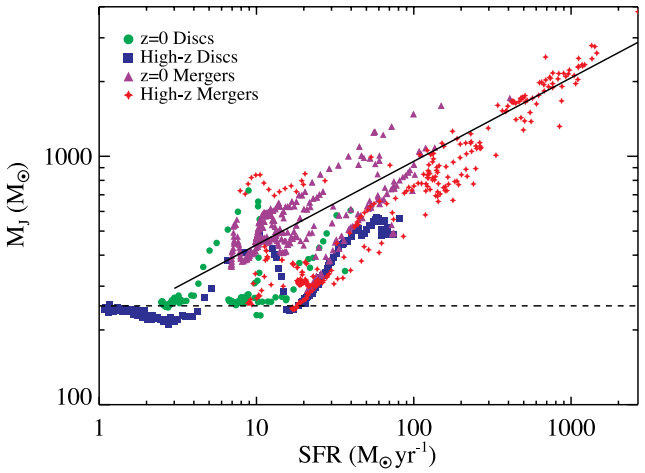

Figure 2. Relationship between SFR and H_2-mass weighted Jeans mass of GMCs for all simulation snapshots in our sample. The points show individual simulation snapshots, and are colour-coded by the type of simulation. The solid line denotes the best-fitting power law, while the dashed line shows a fiducial value of 250 $M_\odot$, the typical Jeans mass for a GMC with density $n \approx 1$–2×10^2 cm^{-3} and temperature $T \approx 10$ K. Because dust and gas heating are dominated by star formation, M_J scales with the SFR. At low SFRs, the mean GMC density drops enough that gas–grain coupling becomes inefficient, and the heating is dominated by cosmic rays. In this regime, the temperatures of the GMCs are roughly constant ($\sim$10 K), as are the Jeans masses.

star formation, as well as high-z discs with more distributed star formation and moderate temperatures.

We choose to parametrize $\hat{M}_J$ in terms of the SFR in order to facilitate the analysis of inferred observed SFRs of high-z galaxies. In principle, one could imagine a relationship between $\hat{M}_J$ and stellar mass. Indeed, broadly, the lower stellar mass galaxies tend to have low $\hat{M}_J$, and vice versa. However, due to similar stellar masses on (e.g.) before and after a starburst event, the scatter in an $\hat{M}_J$–M_* relation is even larger. Similarly, $\hat{M}_J$ may correlate well with the H_2 gas surface density. Indeed, Narayanan et al. (2012) showed that the physical conditions in the gas (temperature and velocity dispersion) scale well with the molecular gas surface density. The scatter in such a relation, however, is similar to the $\hat{M}_J$–SFR relation (the SFR is forced to scale with the volumetric gas density, and shows a tight correspondence with the gas surface density for these simulations; Narayanan et al. 2011a).

One could similarly imagine a Jeans mass that is determined by the median density in the gas, rather than the mean density. As it turns out, this has little effect on our results. We discuss this issue in further detail in Appendix A.

Finally, we emphasize that what governs the Jeans mass in GMCs is the physical conditions in the ISM, and not the global morphology. As such, both heavily star-forming discs (e.g. the *BzK* population at $z \sim 2$) and galaxy mergers may exhibit warmer ISM gas relative to today's discs. One can expect short-lived nuclear starbursts driven by major mergers in the local Universe to exhibit an increase in $\hat{M}_J$ by a factor of $\gtrsim$5. Similarly, high-z disc galaxies that are forming stars at many tens of $M_\odot$ yr^{-1} for a much longer duty cycle may show an increased $\hat{M}_J$ in their GMCs by a factor of $\sim$2–3. The increase in temperature of the ISM is typically driven by warm dust and increasing fractions of molecular gas above the gas–grain coupling density with increasing SFR. We note that very high redshifts, when comparing to galaxies at a fixed density, then the Jeans mass will only scale with the SFR once the mean gas temperature is warmer than the CMB temperature. We discuss this more quantitatively in Section 4.5.

4 IMPLICATIONS FOR OBSERVED STAR FORMATION RATES

We showed that the H_2 mass-weighted Jeans mass can vary substantially in galaxies with physical conditions different from that in the MW. We now make the assumption that variations in $\hat{M}_J$ map directly into variations in the characteristic mass $\hat{M}_c$ of the IMF. This then allows us to investigate how such variations in $\hat{M}_J$ will change the inferred SFRs.

It is useful to parametrize this variation in terms of how the bolometric luminosity L_{bol} varies with SFR. In a star-forming galaxy, L_{bol} is essentially dominated by the emission from high-mass stars. All currently used extragalactic SFR tracers trace such stars. Hence examining the variations in L_{bol} is likely to be broadly representative of the variations that would be seen in any of the canonical SFR tracers. For an invariant IMF, L_{bol} is linearly related to SFR (assuming, as we will throughout, that there is no significant contribution from active galactic nuclei). But when the IMF varies, then L_{bol} will trace only high-mass stars, while the true SFR includes all stars, thereby breaking the linear relation.

To quantify the SFR–L_{bol} relation, we begin by assuming that the IMF has a broken power-law form characterized by a turnover mass, $\hat{M}_c$, a low-mass slope of 0.3, and a high-mass slope of -1.3 [where the IMF slope specifies the slope of the $\log_{10}(dN/d\log M)$–$\log_{10}(M)$ relation]. If $\hat{M}_c$ scales with M_J, then we can calculate the variation in the L_{bol}–SFR relationship as a function of $\hat{M}_c$ by employing stellar population synthesis modelling.

We employ FSPS, a publicly available stellar population synthesis code (Conroy, Gunn & White 2009; Conroy, White & Gunn 2010; Conroy & Gunn 2010). FSPS allows for the quick generation of stellar spectra given a flexible input form for the IMF. We assume a constant star formation history (SFH) of 10 $M_\odot$ yr^{-1}. This was chosen as a reasonable approximation for the SFH of a ($z = 0$) $M_* = 10^{10.5}$ $M_\odot$ galaxy in cosmological simulations (Davé 2008). We additionally assume solar metallicity stars, and include the contribution from thermally pulsating asymptotic giant branch (AGB) stars. No dust extinction is included.

Using FSPS, we find that $L_{bol}/\mathrm{SFR} \sim \hat{M}_c{}^{0.3}$. To test our model assumptions, we vary the assumed SFH and assume a constant SFH of 50 $M_\odot$ yr^{-1}, as well as an exponentially declining SFH with an initial SFR of 50 and 10 $M_\odot$ yr^{-1} and an e-folding time of 10 Gyr. All assumed SFH models return an L_{bol}/SFR–$\hat{M}_c$ exponent within 10 per cent of our fiducial model. Combining our fiducial L_{bol}/SFR–$\hat{M}_c$ relation with the model fit to the SFR–$\hat{M}_c$ relation fit from Fig. 2, we arrive at the relation

$$\mathrm{SFR} = \left[\frac{L_{bol}}{10^{10}\,L_\odot}\right]^{0.88} M_\odot\ \mathrm{yr}^{-1}, \quad \text{for SFR} \gtrsim 3\ M_\odot\ \mathrm{yr}^{-1}. \qquad (4)$$

As can be seen in Fig. 2, at SFR $\lesssim 3$ $M_\odot$ yr^{-1} there is no strong variation of $\hat{M}_J$ with SFR, so in that regime SFR $\propto L_{bol}$.

At Ultraluminous Infrared Galaxy (ULIRG)-type SFRs ($\sim$100 $M_\odot$ yr^{-1}), our model suggests that SFRs may need to be adjusted by a factor of $\sim$2. At the luminosities of distant SMGs, the most luminous, heavily star-forming galaxies in the Universe, typical SFRs may be closer to $\sim$400 $M_\odot$ yr^{-1}, rather than the canonically inferred $\sim$1000 $M_\odot$ yr^{-1}.

Though the correction to the inferred SFRs from a standard Kroupa IMF is relatively mild (only a factor of $\sim$3 at a SFR of $\sim$1000 $M_\odot$ yr^{-1}), the impact on cosmological SFRs can be

substantial owing to the strong evolution of global SFRs. In the following sections, we discuss the impact of a SFR–$L_{\rm bol}$ relation that derives from a variable IMF on the observed KS star formation relation, the SFR–M_* relation, high-redshift SMGs and the observed cosmic SFR density.

4.1 The Kennicutt–Schmidt star formation law

The KS star formation relation is a power-law relationship between the SFR surface density against the gas surface density of both sub-regions of galaxies and galaxies as a whole. A reasonably tight relationship has been observed on scales as small as GMC clumps (Wu et al. 2005, 2010; Heiderman et al. 2010; Lada et al. 2012), $\sim 10^2$–10^3 pc scale regions in galaxies (e.g. Kennicutt 1998b; Bigiel et al. 2008; Schruba et al. 2011) and galaxies as a whole at both low and high z (e.g. Gao & Solomon 2004a,b; Narayanan et al. 2005; Bussmann et al. 2008; Iono et al. 2009; Daddi et al. 2010a; Genzel et al. 2010; Garcia-Burillo et al. 2012). The relationship between the SFR and gas density is crucial both for our understanding of the dominant physical effects in controlling SFRs (e.g. Silk 1997; Elmegreen 2002; Krumholz & McKee 2005; Tan 2010; Ostriker & Shetty 2011, to name just a few), and for input into galaxy evolution simulations (e.g. Springel & Hernquist 2003; Robertson & Kravtsov 2008; Bournaud et al. 2010; Ceverino, Dekel & Bournaud 2010b).

The KS relation is typically measured observationally via a combination of inferred SFRs, and measured H_2 gas masses. At face value, assuming a constant $L_{\rm bol}$–SFR relation, and a constant CO–H_2 conversion factor, a relation $\Sigma_{\rm SFR}$–$\Sigma_{\rm H2}^{1.3-1.5}$ results when including both local and high-z data (e.g. Daddi et al. 2010a; Genzel et al. 2010).[4] However, it is now well established that the CO–H_2 conversion factor is not universal. Observations (e.g. Bolatto et al. 2008; Tacconi et al. 2008; Leroy et al. 2011; Genzel et al. 2012) and theory (Feldmann, Gnedin & Kravtsov 2011; Narayanan et al. 2012; Shetty et al. 2011a,b) motivate a continuous form of $X_{\rm CO}$ in terms of the physical properties of the H_2 gas. Narayanan et al. (2012) derived a functional form for the CO–H_2 conversion factor ($X_{\rm CO}$) as a function of CO surface brightness as an observable proxy for the gas density and velocity dispersion. These authors showed that combining their model of $X_{\rm CO}$ with literature data results in a steeper inferred KS relation, $\Sigma_{\rm SFR} \sim \Sigma_{\rm H2}^2$. This owes to decreasing CO–H_2 conversion factors at higher SFR surface densities, and assumes a linear $L_{\rm bol}$–SFR relation.

If the stellar IMF varies with the physical conditions in the ISM, the KS relation will be further modified, since $L_{\rm bol}$–SFR is no longer linear. Equation (4) suggests when utilizing a standard Kroupa IMF, the inferred SFR for the most heavily star-forming galaxies may be overestimated, and that the KS power-law index will decrease. In Fig. 3, we plot the compiled data from Narayanan et al. (2012), which include both resolved regions from nearby galaxies and global data from quiescent discs and starburst galaxies from $z \approx 0$ to 2, on a KS relation. The data have had their SFRs calculated via equation (4). The best-fitting relation is $\Sigma_{\rm SFR} \sim \Sigma_{\rm H2}^{1.6}$. For reference, we show the Narayanan et al. (2012) relation, $\Sigma_{\rm SFR} \sim \Sigma_{\rm H2}^2$ relation via the blue dashed line.

In order to calculate the modified SFRs in Fig. 3, we assume that the original SFRs reported in the papers that the data originate from are relatable to the $L_{\rm IR}$ via the standard Kennicutt (1998a) relation, and that $L_{\rm bol} \approx L_{\rm IR}$. This is likely a reasonable assumption. Galaxies below SFR of 3 $M_\odot$ yr^{-1} do not undergo a modification to the SFR in our model. The galaxies which will have the strongest modification to their SFR when utilizing our model IMF are those that form stars at the rates of SFR $\gtrsim 100$ $M_\odot$ yr^{-1}. These galaxies are typically mergers in the local Universe, and either heavily star-forming discs or mergers at high z, and the bulk of their luminosity is in the infrared.

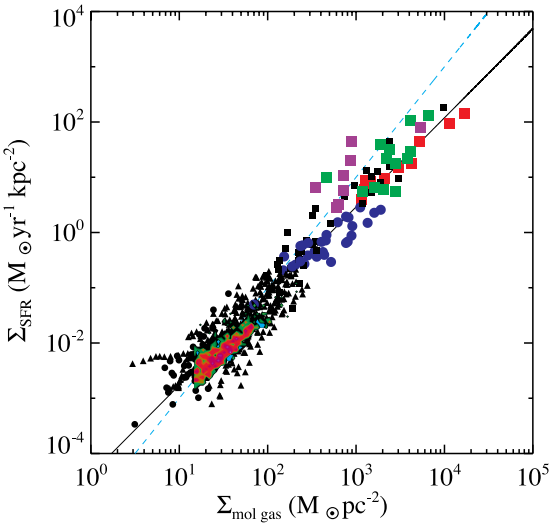

Figure 3. KS $\Sigma_{\rm SFR}$–$\Sigma_{\rm mol}$ star formation law. Solid line shows the relation $\Sigma_{\rm SFR} \sim \Sigma_{\rm mol}^{1.6}$ that results when utilizing the SFR corrections derived for the model IMF in this paper, and the model functional form for the CO–H_2 conversion factor presented in Narayanan et al. (2012). The blue dashed line denotes the relation $\Sigma_{\rm SFR} \sim \Sigma_{\rm mol}^2$, which results if the IMF does not vary with the Jeans mass of GMCs. The low-z data are from Kennicutt et al. (2007), Wong & Blitz (2002), Crosthwaite & Turner (2007), Schuster et al. (2007), Bigiel et al. (2008), Kennicutt (1998b), whereas the high-z data are from Genzel et al. (2010), Daddi et al. (2010a,b), Bothwell et al. (2010), Bouché et al. (2007), Greve et al. (2005), Tacconi et al. (2006, 2008) and Engel et al. (2010).

Any theory that relates the SFR to the free-fall time in a GMC naturally results in a relation SFR $\sim \rho_{\rm H2}^{1.5}$. For galaxies of a constant scale height, this translates into a similar surface density relation. An assumption of a constant scale height across such a wide range of physical conditions is debatable, however (Shetty & Ostriker 2008; Krumholz, Dekel & McKee 2012b). Alternatively, if SFR $\sim \rho$ for quiescent regions, and has a steeper relation for starburst galaxies as expected for a scenario in which gas dominates the vertical gravity (Ostriker & Shetty 2011), then a surface density relation steeper than unity is natural.

4.2 The dynamical time star formation law

As an alternative to the standard KS relation that relates $\Sigma_{\rm SFR}$ to $\Sigma_{\rm H2}$, some theories posit that the gas density divided by the galaxy dynamical time or local free-fall time may be the relevant physical parameter controlling the SFR (e.g. Silk 1997; Elmegreen 2002). It is of interest, therefore, to estimate the modified $\Sigma_{\rm SFR}$–$\Sigma_{\rm H2}/t_{\rm dyn}$ and $\Sigma_{\rm SFR}$–$\Sigma_{\rm H2}/t_{\rm ff}$ relations given our model IMF which varies with the physical conditions in the ISM. We plot these relations in Fig. 4.

Following Daddi et al. (2010a) and Genzel et al. (2010), we define the dynamical time of the galaxies in Fig. 3 as the rotational time either at the galaxy's outermost observed radius or at the half

[4] We note that when considering only local data from quiescent discs, the KS relation has a roughly linear index (Bigiel et al. 2008). It is only when including higher surface-density galaxies such as ULIRGs or high-z galaxies that the fit is torqued towards higher values (Krumholz et al. 2009b).

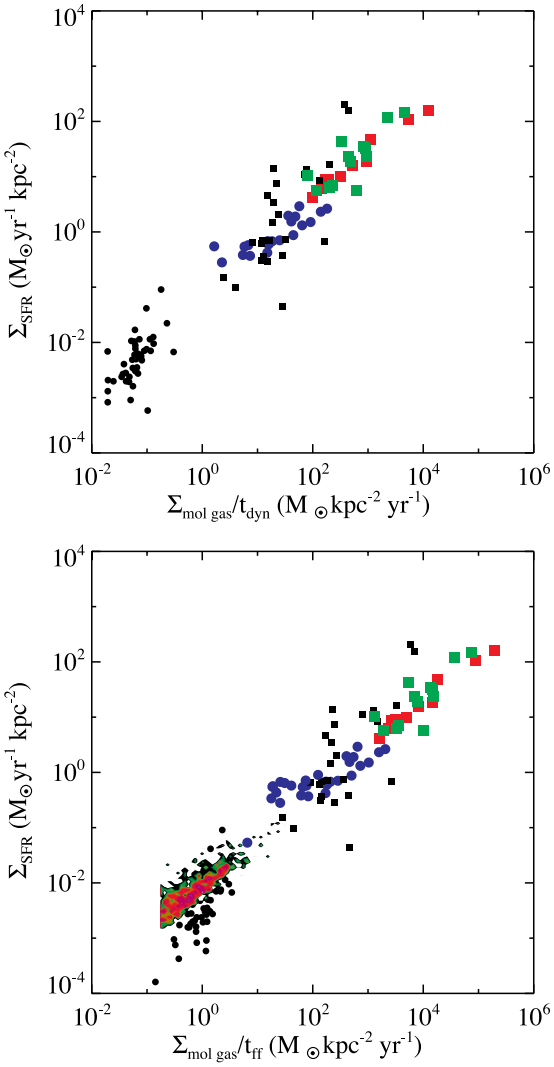

Figure 4. Similar to Fig. 3, but with gas surface densities divided by the dynamical time (top) or free-fall time (bottom). Both relations are nearly linear, with star formation efficiencies $\epsilon_{ff} \sim 0.01$ (see text for details).

light radius, depending on the sample. When assuming a constant SFR–L_{bol} relation,[5] Σ_{SFR} is nearly linearly related to Σ_{mol}/t_{dyn}, with exponent ∼1.03 (Narayanan et al. 2012). When we use equation (4) to calculate the SFRs, a relation $\Sigma_{SFR} \sim \Sigma_{mol}/t_{dyn}^{0.9}$ results. Hence, this IMF-driven variation produces only a minor change to the relation relative to a constant SFR–L_{bol} relation.

Why does this relation change only marginally when the change in the Σ_{SFR}–Σ_{mol} was more pronounced? Σ_{mol}/t_{dyn} spans ∼6 orders of magnitude when considering the galaxies in Fig. 3, whereas Σ_{mol} spans only ∼4. The drop in the SFR of the most heavily star-forming galaxies when assuming our model IMF makes less of an impact on the inferred relation than in the Σ_{SFR}–Σ_{mol} case.

Similarly, we can consider how our model affects the Σ_{SFR}-Σ_{mol}/t_{ff} relation. Both observations and models have suggested that the star formation efficiency per free-fall time should be roughly constant in molecular gas (Krumholz & McKee 2005; Krumholz & Tan 2007; Evans et al. 2009; Ostriker & Shetty 2011; Krumholz, Dekel & McKee 2012a). Following Krumholz et al. (2012a), we infer the free-fall time from the observable properties of the galaxy. Similar to the Σ_{SFR}–Σ_{mol}/t_{dyn} relation, when assuming a constant SFR–L_{bol} relation, Σ_{SFR} varies roughly linearly with Σ_{mol}/t_{ff} (Narayanan et al. 2012). Introducing a variable IMF in the SFR calculations results in a moderate change in the Σ_{SFR}–Σ_{mol}/t_{ff} exponent to ∼0.9 for similar reasons as in the t_{dyn} calculation. A star formation efficiency $\epsilon_{ff} \approx 0.01$ provides a good fit to the relation $\Sigma_{SFR} = \epsilon_{ff}\Sigma_{mol}/t_{ff}$.

4.3 The SFR–M_* relation

The stellar masses and SFRs of galaxies have been observed to have a relatively tight relationship as early as $z = 6$–8 (Daddi et al. 2007; Noeske et al. 2007a,b; Stark et al. 2009; McLure et al. 2011). The SFR–M_* relation appears to steadily decrease in normalization with time, in accordance with cosmological simulations that suggest that star formation is fuelled by gravitational infall of baryons into the galaxy (e.g. Kereš et al. 2005; Davé et al. 2011), which shows a rapid drop with redshift (e.g. Dekel et al. 2009b).

As alluded to in Section 1, while simulations predict the slope and scatter of the SFR–M_* relation with reasonable success, the amplitude at $z \approx 2$ is less well reproduced. In models, the SFRs at a given M_* at $z = 2$ are too low by two to three times compared with observations. This is a fairly small discrepancy given the systematic uncertainties, but is nonetheless persistent for simulations performed via a variety of techniques (hydrodynamic simulations performed using SPH or adaptive mesh refinement, as well as SAMs).

This discrepancy led Davé (2008) to suggest that perhaps the SFRs of $z \sim 2$ galaxies are overestimated. Davé empirically derived an IMF that varies its critical mass with redshift as $\hat{M}_c = 0.5(1 + z)^2\ M_\odot$ for $0 < z < 2$ as being able to reconcile the models and data. Our model for a varying IMF differs from the Davé (2008) model in that here the IMF varies with the temperature and density of GMCs in the ISM, rather than with redshift. Thus, a heavily star-forming galaxy in the local Universe may have an IMF more comparable to a luminous disc at $z \sim 2$ than a present-epoch quiescent disc. Nevertheless, the impact of such a varying IMF does imply a strong dependence in redshift because high-redshift galaxies form stars far more rapidly.

In Fig. 5, we plot the observed SFR–M_* data from the Sloan Digital Sky Survey (SDSS; $z = 0$) and Great Observatories Origins Deep Survey (GOODS; $z = 1$–2), overlaid by the predicted SFR–M_* relation from simulated galaxies drawn from the hydrodynamic cosmological simulations of Davé et al. (2011). The left-hand panel shows the observed and modelled SFR–M_* relation assuming a Kroupa IMF with turnover mass $\hat{M}_c = 0.5\ M_\odot$. With increasing redshift, the discrepancy between the normalization of the observed SFR–M_* relation and modelled one grows, becoming noticeable at $z \gtrsim 1$.

If the turnover mass in the IMF varies with the Jeans mass in GMCs, this discrepancy may be ameliorated. Turning now to the right-hand panel, we show the same comparison after correcting the SFRs via equation (4). While the relatively quiescent galaxies in the observed low-z samples undergo relatively little correction to their already modest SFRs, the galaxies at high z tend to be brighter at a given stellar mass than their low-z counterparts due to increased gas fractions and densities. The SFRs for these galaxies undergo a larger correction per equation (4), and bring the observed SFR–M_* relation into agreement with simulations.

[5] Note that this relation depends on the usage of a physically motivated functional form for the CO–H_2 conversion factor that depends on the CO surface brightness and the metallicity of the galaxy (Narayanan et al. 2012).

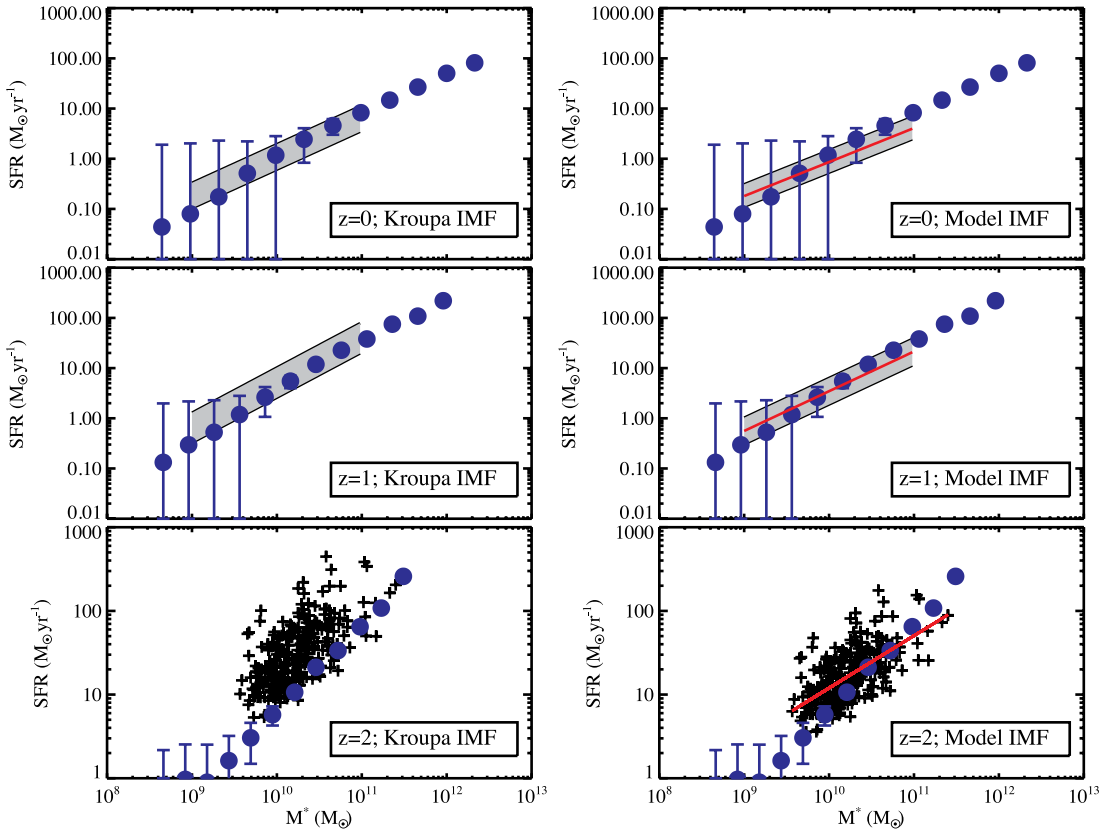

Figure 5. SFR–M_* relationship for $z = 0$, 1, 2 galaxies. Left-hand panels are literature values of SFR, and right show corrected SFRs using our model IMF. In the top two rows, the shaded grey region shows the median observed relationship from Elbaz et al. (2007), with dispersion, and in the bottom row the crosses come from Daddi et al. (2007). In all panels, the circles with error bars show the simulated points from Davé et al. (2011) in bins of M_*, with dispersion. The red lines in the right-hand panel show the best fit to the modified SFR–M_* relation. When using a standard Kroupa IMF, the simulated galaxies underpredict the SFRs by as much as a factor of ∼10. When assuming an IMF that scales with the thermal conditions in the molecular ISM, the simulated SFR–M_* relation and observed one comes into much better agreement. This is most apparent in the $z = 2$ case (bottom row).

We fit a power-law form to observations, as reinterpreted using our evolving IMF. For the $z = 0$ and $z = 1$ data, we fit the change in the median relations reported by Elbaz et al. (2007). For the $z = 2$ data, we perform a polynomial fit to the data from Daddi et al. (2007).[6] Our best-fitting relations are

$$(z = 0) : \mathrm{SFR}(\mathrm{M}_\odot\ \mathrm{yr}^{-1}) = 3.9 \times \left[\frac{M_*}{10^{11}\ \mathrm{M}_\odot}\right]^{0.65} \quad (5)$$

$$(z = 1) : \mathrm{SFR}(\mathrm{M}_\odot\ \mathrm{yr}^{-1}) = 19.3 \times \left[\frac{M_*}{10^{11}\ \mathrm{M}_\odot}\right]^{0.77} \quad (6)$$

$$(z = 2) : \mathrm{SFR}(\mathrm{M}_\odot\ \mathrm{yr}^{-1}) = 50.2 \times \left[\frac{M_*}{10^{11}\ \mathrm{M}_\odot}\right]^{0.55} \quad (7)$$

and are denoted in Fig. 5 by the solid red lines in the right-hand panel.

It important to note that all of these relations should be regarded as tentative – they represent relatively limited ranges of stellar masses, and for the $z = 0$ and $z = 1$ data the relations were derived by re-fitting published fits, not the actual data with error bars. This is therefore only intended to be illustrative of the sense and magnitude of the changes in SFR–M_* when applying an IMF with $\hat{M}_c \propto \hat{M}_J$.

[6] Note that we do not have error bars available for the Daddi et al. (2007) data.

The best-fitting exponents for $z = [0,1,2]$ as reported by Daddi et al. (2007) and Elbaz et al. (2007) are ∼[0.77, 0.9, 0.9], respectively, which in our scenario decrease to ∼[0.65, 0.77, 0.55]. This, of course, owes to the fact that in our model, galaxies with larger inferred SFRs (using a standard Salpeter or Kroupa IMF) undergo a larger correction to their SFR when the IMF varies with the Jeans mass. Similarly, the amplitudes of the SFR–M_* relations in Fig. 5 are lower than previously estimated due to lower SFRs.

The cosmological simulation predictions now match the observations quite well in amplitude (around $\sim L^*$), but the slope is now more discrepant. A selection effect that could explain this discrepancy is that low SFR galaxies tend to be absent from these samples, creating a floor in observed SFRs that increases to higher redshifts. Combined with the (not insubstantial) scatter in the SFR–M_* relation, this could induce a shallower observed slope relative to the true slope (Reddy et al., in preparation). On the other hand, it could also just indicate a failing in these simulations. We leave a more detailed comparison to models for a later time (since in detail, an evolving IMF would have secondary implications for galaxy evolution in these models that are not accounted for by this simple rescaling). For now, we simply illustrate how galaxy SFRs could be significantly lowered by an evolving IMF during the peak epoch of cosmic star formation.

An important constraint on SFR–M_* evolution is that its amplitude appears to be essentially constant from $z \sim 2$ to 6 (Stark et al. 2009; Bouwens et al. 2011). Simulations, on the other hand, tend to

predict an amplitude that continues to rise, albeit at a slower pace than at lower redshifts. Hence as discussed in Davé (2011), if the IMF varies in some systematic way with redshift in order to reconcile models and data, then the evolution must *reverse* at higher redshifts. This would require that the typical SFRs of galaxies at $z \gtrsim 2$ should be lower at earlier epochs. Such an evolution is at least qualitatively consistent with the observation that L^* decreases going to higher redshifts (i.e. the Universe is 'upsizing' at that early epoch, not downsizing). On the other hand, at very high redshifts, the CMB temperature rises accordingly, setting a larger minimum ISM temperature (and hence a larger minimum Jeans mass). In this sense, it is not quite obvious how to reconcile the potential discrepancy between the observed normalization of the SFR–M_* relation and modelled one. A quantitative comparison will require a more thorough analysis of the data versus the models, which we leave for the future.

4.4 Sub-millimetre galaxies

SMGs at high redshifts are the most rapidly star-forming galaxies known, and hence likely represent an extreme of ISM physical conditions where our IMF scenario would predict the largest variations. Indeed, theoretical models attempting to reproduce SMGs have sometimes resorted to invoking IMF variations in order to explain these systems.

SAMs with a canonical IMF have difficulty matching the number counts of high z infrared and sub-millimetre luminous galaxies (Baugh et al. 2005; González et al. 2011; Niemi et al. 2012), and have invoked as a solution that the IMF is more top-heavy in these merger-driven starbursting systems. On the other hand, the required IMF variation in this scenario is rather extreme, namely a flat IMF above $1\,\mathrm{M}_\odot$, which is disfavoured by observational constraints on the IMF from measuring the gas, stellar and dynamical mass of SMGs (Tacconi et al. 2008).

The simulations of Davé et al. (2010) suggest a different origin for SMGs, as the high-mass, high-SFR end of the $z \sim 2$–3 galaxy main sequence. While these models can broadly reproduce many properties of SMGs, they do not achieve the high SFRs inferred from the SMG observations, falling short by a factor of $\sim$3. This is similar to the correction factor predicted in equation (4) for the most IR luminous galaxies. Hence if the IMF varied in the manner considered here, this scenario for the origin of SMGs would be strengthened.

Conversely, recent hydrodynamic simulations of isolated galaxies and galaxy mergers (similar to those presented here), coupled with dust radiative transfer calculations and semi-empirical cosmological simulations, have shown that the number counts of high-z sub-millimetre selected galaxies may be accounted for while utilizing a Kroupa IMF (Hayward et al. 2010, 2011; Narayanan et al. 2010), at least within the current uncertainties. These models suggest that pairs of galaxies blended within a single far-IR beam may be an important observational bias at lower flux densities, and that the relationship between sub-millimetre flux density and SFR may not be linear owing to substantial variations in dust temperatures during the merger phase. If the observed number counts from upcoming surveys turn out to be in good agreement with these predictions at a range of far-IR wavelengths, then an IMF-based solution may be unnecessary.

While they differ in detail, both the Davé et al. (2010) and Hayward et al. (2011) models suggest that the lowest luminosity SMGs ($F_{850} \sim 5\,\mathrm{mJy}$) galaxies may represent individual, heavily star-forming discs, whereas more luminous SMGs likely owe their origin to galaxy mergers. In hydrodynamic cosmological simulations, individual discs rarely sustain SFRs at rates larger than $\sim 500\,\mathrm{M}_\odot\,\mathrm{yr}^{-1}$ (Dekel et al. 2009b; Davé et al. 2010; Hayward et al. 2011). Utilizing equation (4), this corresponds to luminosities $L_{\rm bol} \approx 10^{13}\,\mathrm{L}_\odot$, and may reflect a transition luminosity where objects above this are typically mergers at $z \sim 2$. Recent analysis of the specific SFRs and $L_{\rm IR}$–$T_{\rm dust}$ relation for high-z SMGs by Magnelli et al. (2012) suggests that this may indeed represent a transition luminosity between galaxy populations. At $L_{\rm bol} \approx 10^{13}\,\mathrm{L}_\odot$, the $L_{\rm IR}$–$T_{\rm dust}$ relation steepens dramatically, and galaxies rise above the 'main-sequence' of specific SFRs at $z \sim 2$ (Daddi et al. 2007; Rodighiero et al. 2011). Moreover, models by Hopkins et al. (2010) show that $L_{\rm bol} \approx 10^{13}\,\mathrm{L}_\odot$ represents a transition luminosity above which the luminosity function is dominated by mergers at $z \sim 2$. If a Salpeter IMF holds for $z \sim 2$ SMGs, an SFR of $500\,\mathrm{M}_\odot\,\mathrm{yr}^{-1}$ would correspond to $\sim 3 \times 10^{12}\,\mathrm{L}_\odot$, an implausibly low transition luminosity given $z \sim 2$ merger rates (Fakhouri & Ma 2008; Guo & White 2008; Hopkins et al. 2010).

In short, achieving the extreme SFRs inferred for SMGs at their observed number densities using a canonical IMF remains a challenge for hierarchical-based models. While observations are sufficiently uncertain to be broadly consistent with a variety of scenarios, tensions could generally be alleviated if the SFRs were a factor of several lower in these systems as would be the case for the varying IMF presented here. Our model form for the IMF suggests a reasonable transition luminosity for the break between discs and mergers at $z \sim 2$, given a rough maximal SFR for a quiescent disc of $\sim 500\,\mathrm{M}_\odot\,\mathrm{yr}^{-1}$ ($L_{\rm bol} \approx 10^{13}\,\mathrm{L}_\odot$).

4.5 The evolution of cosmic star formation rate density

Deep surveys have permitted measurements of the evolution of the SFRs per unit volume over cosmic time. Similarly, increased sensitivities in the near-infrared have allowed for a more robust reconstruction of the global stellar mass evolution in galaxies out to $z \sim 3$. In principle, the integral of the SFR density, corrected for stellar mass loss, should be equivalent to the stellar mass density at a given redshift. A number of authors have noted, however, that there may be a discrepancy between these two quantities, such that the cosmic SFR density appears to be overestimated (Hopkins & Beacom 2006; Pérez-González et al. 2008; Wilkins et al. 2008). As alluded to in Section 1, an IMF weighted towards more high-mass stars at high z may go some length towards solving this issue.

Does an IMF that varies with the Jeans mass of GMCs reduce the inferred SFRs of high-z galaxies enough to remove the discrepancy between the integrated SFR density and the observed stellar mass density? To answer this, we need to determine how a varying IMF would impact the inferred global SFR density. To do this, we employ a functional form for the observed luminosity function of galaxies as a function of redshift that is quite successful in matching existing data from Hopkins et al. (2010). We integrate this functional form as a function of luminosity to calculate the typical number of galaxies per Mpc^3 as a function of redshift (integrated to $0.1L^*$). We similarly utilize this information to calculate a luminosity and SFR density as a function of redshift. This information combined with the average number density of galaxies as a function of redshift allows us to calculate the typical SFR per galaxy as a function of redshift. We then apply the correction given in equation (4) after converting to an infrared luminosity via the Kennicutt (1998a) relations, and assuming $L_{\rm IR} \approx L_{\rm bol}$.

Fig. 6 shows the resulting Star Formation Rate Density (SFRD) evolution assuming an unevolving Kroupa IMF (purple), versus

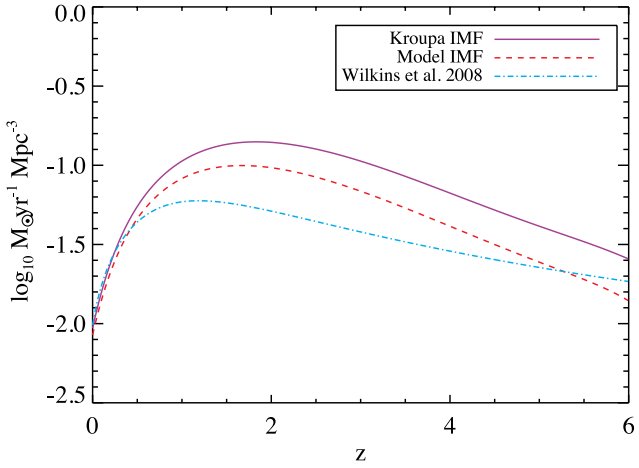

Figure 6. Evolution of cosmic SFR density. The purple solid line shows model form from Hopkins et al. (2010), assuming a Kroupa IMF. This provides a good fit to the observed SFR density measurements of Hopkins & Beacom (2006). When applying our model form for IMF variations, the SFR density decreases, as is shown by the red dashed line. The blue dash–dotted line shows the Wilkins et al. (2008) SFR density that would be necessary to match the observed present-day stellar mass density. The application of our model IMF decreases the inferred SFR density. But because much of the star formation occurs in lower-luminosity systems where the IMF is not substantially different from canonical, the amount of the decrease is not quite enough to account for the discrepancy between the integrated SFR density and stellar mass density as presented in Wilkins et al. (2008).

the model evolving IMF assuming $M_c \propto \hat{M}_J$ (red dashed). The unevolving IMF curve is in good agreement with the SFRD compilation by Hopkins & Beacom (2006) when corrected to a Kroupa IMF; for clarity, we do not show the individual data points. While the evolving IMF makes a large difference to the SFRs of very rapidly star-forming galaxies, the global effect is less dramatic, since the SFRD tends to be dominated by more modestly star-forming systems. Nonetheless, it is clear that it lowers the SFRD significantly at all $z \gtrsim 1$.

Wilkins et al. (2008) suggested a variable IMF that was empirically constructed to reconcile the cosmic SFRD evolution with the present-day stellar mass density. The resulting SFRD evolution in this model is shown as the blue dot–dashed line in Fig. 6. The IMF model presented here results in less of a correction to the present-day stellar mass, since it is clearly closer to the original unevolving case over much of cosmic time. Hence, it remains to be seen if the IMF model in this work can actually reconcile these measurements, although it is clear that it goes some distance towards this. The standard Kroupa IMF forms roughly twice as many stars today as are accounted for in stellar mass density measurements, whereas our model IMF forms 1.3 times the Wilkins et al. estimate.

This said, an evolving IMF is not necessary to reconcile the differences between the cosmic SFRD evolution and stellar mass density. For example, utilizing cosmological SPH simulations, Choi & Nagamine (2012) suggest that the two can come into better agreement if the stellar mass density measurements are missing faint, low-mass galaxies. Similarly, Reddy & Steidel (2009) have suggested that the evolution of the stellar mass density and integral of the cosmic SFR density may not be discrepant. They argue that if one integrates the luminosity function to a common limit (accounting for the evolution of L^* with z), then some of the observed discrepancy between the star SFRD and stellar mass density can be removed.

Overall, the global SFR density is less affected by our model IMF than the most rapidly star-forming galaxies, since much of the global star formation occurs in modestly star-forming systems. Our model IMF goes some of the way towards alleviating the putative discrepancy between the integrated cosmic SFRD and the global stellar mass evolution, although current observations still disagree on the magnitude of the discrepancy.

Finally, we note that the rising CMB temperature with redshift sets an increasing minimum Jeans mass that is non-negligible at large ($z \gtrsim 3$) redshifts. However, due to the rising SFR per galaxy with redshift, the average conditions are already warm enough due to gas-dust coupling that the effect of the CMB is negligible. As an example, at $z \sim 4$, the CMB temperature is $\sim$15 K. The mean SFR per galaxy is $\sim 20\,M_\odot\,yr^{-1}$, which corresponds to a typical gas temperature of $\sim$20 K (see e.g. Fig. 1).

5 DISCUSSION

5.1 Arguments for and against a varying IMF

Probably the single greatest piece of evidence for an invariant IMF is that no conclusive evidence for a varying IMF has ever been seen, even when probing a fairly wide range of physical conditions and environments in star-forming regions within the MW and nearby galaxies. For this reason as well as others, all arguments for a varying IMF must be taken with a healthy degree of scepticism. The recent review by Bastian et al. (2010) takes a rather critical view of observational claims of IMF variations; we refer the reader there for a fuller discussion.

There are many theoretical studies that suggest that the IMF should be essentially constant in most relevant regimes. Krumholz (2011) present a model in which the temperature in typical star-forming regions in GMCs is set by radiation feedback from accretion on to protostars. In this scenario, one can arrive at a characteristic stellar mass primarily via fundamental constants, with only weak scaling with the physical properties of the GMC. Similar arguments were made by Bate (2009). This theory may explain the near constancy of the IMF in normal star-forming regions in the Galaxy, and has the additional attractive aspect of explaining why stars form to massive enough scales to begin hydrogen fusion.

On the other hand, there have been a number of recent claims that the IMF varies with galaxy properties. It is now reasonably well established that the Hα to UV luminosity ratio varies systematically with luminosity (Hoversten & Glazebrook 2008), SFR (Lee et al. 2009) and/or surface brightness (Meurer et al. 2009), in the sense that for fainter galaxies there is less Hα than expected given the UV luminosity. Since Hα traces very high mass stars while UV traces moderately high mass stars, one possible explanation is that smaller GMCs are unable to produce very high mass stars. In this scenario, fainter systems with on average smaller GMCs would have an integrated galactic IMF that is less top-heavy. This variation would work in the same direction as the IMF variations considered in this paper (i.e. more top-heavy/bottom-light in more rapidly star-forming systems), but for a different reason; also, it is seen to operate down to very low SFRs (and indeed it is most evident there), whereas our results suggest that IMF variations based on the Jeans mass conjecture have little impact at SFRs of the MW or smaller. That said, numerous investigations recently have discussed other physical effects that could lead to the observed trends in Hα/UV, such as the leakage of ionizing photons, stochasticity in the formation of the most massive stars (Fumagalli, da Silva & Krumholz 2011), variable star formation histories (Weisz et al. 2012) and

extinction effects. Similarly, studies investigating the production rate of ionizing photons in stellar clusters (Calzetti et al. 2010), as well as outer galaxy discs (Koda et al. 2012), find no evidence for a varying IMF. Hence while intriguing, Hα/UV variations are not widely considered to be an unambiguous indication of a varying IMF.

Early-type galaxies also show tantalizing hints for IMF variations. van Dokkum & Conroy (2011) observed the Wing-Ford absorption bands (tracing stellar masses $\lesssim 0.3\,M_\odot$) in nearby cluster elliptical galaxies, and found that they indicate a much larger population of low-mass stars than expected from a Galactic IMF, i.e. that the IMF in these galaxies is bottom-heavy. Cappellari et al. (2012) did careful dynamical modelling of ellipticals from the ATLAS-3D sample, and showed that high-mass ellipticals tend to have such mass-to-light ratios (*M/L*) that they can only be explained by a bottom-heavy IMF. They also found a strong trend of IMF variation with *M/L*. These data argue for a bottom-heavy IMF as opposed to a bottom-light one as considered in this paper, but a naive extrapolation of their trend with *M/L* suggests that rapidly star-forming systems may have a top-heavy/bottom-light IMF. However, it is also expected that massive star-forming systems at high z should evolve into present-day passive ellipticals, and thus it is not immediately clear how to reconcile these differing IMFs within a single galaxy evolution scenario. If, indeed, the IMF is bottom-heavy in the progenitor galaxies of present-day ellipticals, then this likely rules out the model presented in this paper (van Dokkum 2008; Cappellari et al. 2012; Conroy & van Dokkum 2012).

If the IMF is indeed invariant, then what about the cosmic star formation problems discussed throughout this work? There are certainly solutions that do not require an IMF-based solution. There are many well-documented systematic uncertainties associated with measuring SFRs and M_*, particularly at high redshifts when only broad-band data are available (e.g. Shapley et al. 2005). It is not difficult to imagine that one or more of these could alleviate the apparent discrepancies (see a discussion in Davé 2008). There could also be failures in current modelling techniques or assumptions. For instance, the high specific star formation rate (sSFR) of $z \sim 2$ galaxies could owe to a strong inefficiency of star formation in earlier galaxies owing, e.g., to lower metallicities (Gnedin & Kravtsov 2010; Bolatto et al. 2011), resulting in an accumulated gas reservoir that fuels excess star formation at $z \sim 2$ (Krumholz & Dekel 2011). This would not alleviate differences between the observed cosmic SFR and M_* buildup, but perhaps those could be explained by other systematics; for instance, if the bottom-heavy IMF seen in early-type galaxies is real, the total cosmic stellar mass in this component may be underestimated. Finally, it is worth noting that numerical uncertainties still abound in modelling galaxy formation: for instance, Keres et al. (2011) found that SFRs in ($\sim L^*$) galaxies modelled with the moving-mesh code AREPO are a factor ∼2–3 greater than those modelled using the SPH code GADGET-3. With all the various factor-of-2 uncertainties in play, it is difficult to argue strongly for IMF variations as being the only viable solution to any given problem.

As discussed in Section 4.1, a varying IMF may bring the observed KS relation index down from ∼2 to ∼1.5, in agreement with most models which suggest a SFR regulated by dynamical processes. However, as shown by Ostriker & Shetty (2011), if the SFR is instead regulated by supernovae-driven turbulence in a medium where the vertical pressure is dominated by gas, then one would expect a KS index of ∼2. In this sense, even the reduction of the observed KS index is not reason enough to require a variable IMF.

5.2 Arguments for and against the Jeans mass conjecture

In this work, we make the assumption that the IMF characteristic mass scales as the GMC Jeans mass. Here we discuss arguments in favour of and against this Jeans mass conjecture.

Stars form in dense cores in GMCs (e.g. Evans 1999; Lada & Lada 2003) that appear to have a mass function similar in shape to the stellar IMF (Andre, Ward-Thompson & Motte 1996; Johnstone et al. 2001; Motte et al. 2001; Nutter & Ward-Thompson 2007). This suggests that stars acquire their mass from the cores they are born in, and are thus plausibly dependent on the fragmentation scale of the cloud. In the same vein denser(less-dense) clouds, which would have a lower(higher) Jeans mass given the $M_{\rm J} \sim T^{3/2}/n^{1/2}$ scaling, should have a more bottom-heavy(bottom-light) IMF. Observations of the Taurus star-forming region and Orion nebula Cluster provide some evidence of this effect (Briceño et al. 2002; Luhman et al. 2003; Luhman 2004; Da Rio et al. 2012).

Numerical calculations also suggest that the number of fragments that form in a GMC is related to the number of Jeans masses available (Bate & Bonnell 2005). Klessen, Spaans & Jappsen (2007) showed via numerical simulation that warm gas comparable to what may be found in nuclear starbursts indeed forms a mass spectrum of collapsed objects with an $\hat{M}_{\rm c} \approx 15\,M_\odot$, though the degree of fragmentation can depend on the exact form of the equation of state of the gas. It should be noted that observations of the Arches (Kim et al. 2006) and Westerlund 1 clusters (Brandner et al. 2008; Gennaro et al. 2011), regions similar to those in the simulations of Klessen et al. (2007), show minimal evidence for a varying IMF.

Elmegreen, Klessen & Wilson (2008) asked, given cooling rates by molecular lines, and heating rates by dust–gas energy exchange in dense gas, how should $M_{\rm J}$ scale with density? These authors find a weak dependence of the Jeans mass on the density as $n^{1/4}$. Examining Fig. 1, the mass-weighted mean density of GMCs is $\sim 10^4\,{\rm cm}^{-3}$ during the starburst, compared to a few $\times 10^1\,{\rm cm}^{-3}$ during quiescent mode. Following the Elmegreen et al. scalings,[7] this alone would lead to an increase in Jeans mass of ∼4. In other words, even with a relatively weak scaling of $M_{\rm J}$ with density, the conditions inside nuclear starbursts are extreme enough to result in variations in the GMC physical properties as found in our models.

A more general argument against the conjecture that $\hat{M}_{\rm c} \propto \hat{M}_{\rm J}$ is that the choice for the density that sets the Jeans mass is not obvious. In this work we sidestep this problem by considering only how $M_{\rm J}$ scales with galaxy properties and assuming that $\hat{M}_{\rm c} \propto \hat{M}_{\rm J}$ without worrying about the constant of proportionality. However, using typical numbers from our simulations results in $M_{\rm J} \sim 250\,M_\odot$ for the MW (Fig. 2), which is unsatisfyingly far from $\hat{M}_{\rm c} \approx 0.5\,M_\odot$. Larson (2005) assumes that the characteristic density is set when the gas becomes thermally coupled to the dust, and argued against this scale being set by turbulent or magnetic pressure. But in Krumholz (2011) and other recent models, the density where isothermality is broken is set instead by radiative feedback, and thus the IMF characteristic mass is not directly related to the Jeans mass. We note that even if the $\hat{M}_{\rm c}$ is set by radiative feedback, the interstellar radiation properties vary substantially among our various simulated galaxies, and hence there may still be some IMF variations predicted in such a model. Nonetheless, the physical origin of the IMF characteristic mass remains uncertain, and it is by no means entirely clear that it is directly related to the typical GMC Jeans mass.

[7] Note that a similar scaling relation comparing to the global SFR is non-trivial to derive. This depends on radiative transfer processes as well as potential contribution to the radiation field from old stellar populations.

In this paper we suggest that heating of H_2 gas by young stars formed during rapid star formation may increase the Jeans mass. Other models find similar results, though via different heating mechanisms. Papadopoulos (2010) find that the cosmic ray energy densities in starburst environments may be increased, leading to warmer gas kinetic temperatures of the order of ∼80–160 K. Papadopoulos et al. (2011) find that this can lead to increased Jeans masses up to a factor of ∼10. The relevant physical processes in the Papadopoulos model are different from those presented in our work. In a scenario where cosmic rays dominate the heating, the gas and dust do not necessarily have to be thermally coupled. Nevertheless, the results are quite similar to what is found in our study. In Narayanan et al. (2012), we found that even when assuming a cosmic ray flux that scales linearly with the SFR, the heating of dust (and subsequent dust–gas energy exchange at high densities) by young stars in starbursts tends to dominate the heating of the gas. Similarly, Hocuk & Spaans (2010, 2011) have suggested that a strong X-ray field in the vicinity of an accreting black hole may impact the fragmentation length of GMCs, weighting the clump mass spectrum towards higher masses. This scenario is likely to be most relevant in rather extreme cases (e.g. near an AGN), and not necessarily representative of quiescently star-forming galaxies.

Overall, whether the stellar IMF varies in space and/or time and how remains an open question. Strong IMF variations are clearly disallowed by observations, but mild variations may still be accommodated within current constraints. The Jeans mass conjecture is by no means unassailable, and the resulting mild variations in the IMF are probably difficult to exclude given current data.

6 SUMMARY

We use hydrodynamic galaxy evolution simulations and sophisticated radiative transfer models to study how the IMF might vary with galaxy properties, under the assumption that the IMF characteristic mass scales with the H_2 mass-weighted Jeans mass in the ISM. We find that such an assumption results in a typical Jeans mass that varies mildly with SFR, roughly as $\hat{M}_{\rm J} \propto {\rm SFR}^{0.4}$ at SFRs above that of the MW. At SFRs comparable to and lower than that of the MW, there is little variation in $\hat{M}_{\rm J}$ in our model because cosmic ray heating begins to dominate over dust heating, setting a temperature floor at ∼8 K. While this variation is not strong, it is still substantial enough to impact the inferred properties of rapidly star-forming galaxies.

We parametrize the implied IMF variation by considering its impact on SFRs derived from bolometric luminosities. We find that the relation is well-fitted by ${\rm SFR} = (L_{\rm bol}/10^{10}\,{\rm L}_{\odot})^{0.88}$, as opposed to a linear relationship between these quantities as for an invariant IMF (assuming that any AGN contribution has been excluded). Since all extragalactic SFR tracers attempt to measure $L_{\rm bol}$, either directly in the infrared, via a dust-corrected UV continuum, or via nebular emission line measures, this would imply that their inferred SFRs should be lowered in more luminous (i.e. more rapidly star-forming) systems. For instance, in SMGs that are the most bolometrically luminous systems in the Universe, the inferred SFRs would be up to a factor of 5 lower than implied by canonical conversion factors. Large, rapidly star-forming discs at high redshifts would have their inferred SFR lowered by a factor of 2.

We study the impact of such an IMF variation on a variety of galaxy properties across cosmic time. These include the star formation law, the SFR$-M_*$ relation (i.e. the galaxy main sequence), SMGs and the evolution of the cosmic SFR density. In each case, previous work has highlighted tantalizing albeit inconclusive evidence for discrepancies between models and data, or between SFR and stellar mass data. The discrepancies (if real) all point in the same direction, in the sense that the SFR inferred from high-mass tracers seems to exceed the observed growth in stellar mass by approximately two to three times during the peak epoch of cosmic star formation. In each case, the varying IMF based on the Jeans mass conjecture tends to go towards reconciling the possible discrepancies. We caution that there is no smoking gun evidence for IMF variations, and there are numerous ways these discrepancies may be alleviated without varying the IMF. Nonetheless, it is interesting that the ansatz of $\hat{M}_{\rm c} \propto \hat{M}_{\rm J}$ makes measurably different predictions for the evolution of galaxies across cosmic time in a manner that, at face value, tends to reconcile any possible discrepancies.

We remain agnostic on the validity of our underlying assumption, namely the Jeans mass conjecture, and we do not assert that IMF variations are the only solution to the problems discussed here. Rather, this paper merely explores the ansatz that $\hat{M}_{\rm c} \propto \hat{M}_{\rm J}$, and then examines its effects on the SFRs across cosmic time. As we discussed in Section 5, current models for the origin of the IMF characteristic mass are mixed on whether this assumption is correct; a recent class of successful models argues that $\hat{M}_{\rm c}$ is set by radiative feedback in the ISM, not $\hat{M}_{\rm J}$. We leave further explorations along these lines to a different class of models that focus on the origin of the IMF. Additionally, such an evolving IMF would have a wider range of impacts than explored here, owing to differences in, e.g., stellar mass return, metallicity and population synthesis that have not been fully accounted for here. Also, at a constant ISM density, the rising CMB temperature will force increasingly higher Jeans masses with redshift, further complicating matters. Investigating these effects would require running simulations that self-consistently model all these processes during their evolution, which is something we leave for the future.

ACKNOWLEDGMENTS

The authors thank Mark Krumholz for comments on an early version of this draft, and Charlie Conroy, Emanuele Daddi, Dusan Keres, Naveen Reddy and Youngmin Seo for helpful conversations. This work benefited from work done and conversations had at the Aspen Center for Physics. DN acknowledges support from the National Science Foundation via grant number AST-1009452. RD was supported by the National Science Foundation under grant numbers AST-0847667 and AST-0907998. Computing resources were obtained through grant number DMS-0619881 from the National Science Foundation.

REFERENCES

Agertz O., Teyssier R., Moore B., 2011, MNRAS, 410, 1391
Andre P., Ward-Thompson D., Motte F., 1996, A&A, 314, 625
Bastian N., Covey K. R., Meyer M. R., 2010, ARA&A, 48, 339
Bate M. R., 2009, MNRAS, 392, 1363
Bate M. R., Bonnell I. A., 2005, MNRAS, 356, 1201
Baugh C. M. et al., 2005, MNRAS, 356, 1191
Bell E. F., Zheng X. Z., Papovich C., Borch A., Wolf C., Meisenheimer K., 2007, ApJ, 663, 834
Bigiel F., Leroy A., Walter F., Brinks E., de Blok W. J. G., Madore B., Thornley M. D., 2008, AJ, 136, 2846
Bolatto A. D., Leroy A. K., Rosolowsky E., Walter F., Blitz L., 2008, ApJ, 686, 948
Bolatto A. D. et al., 2011, ApJ, 741, 12
Bothwell M. S. et al., 2010, MNRAS, 405, 219

Bouché N. et al., 2007, ApJ, 671, 303
Bournaud F., Elmegreen B. G., Teyssier R., Block D. L., Puerari I., 2010, MNRAS, 409, 1088
Bouwens R. J. et al., 2011, preprint (arXiv:1109.0994)
Brandner W., Clark J. S., Stolte A., Waters R., Negueruela I., Goodwin S. P., 2008, A&A, 478, 137
Briceño C., Luhman K. L., Hartmann L., Stauffer J. R., Kirkpatrick J. D., 2002, ApJ, 580, 317
Bullock J. S., Kolatt T. S., Sigad Y., Somerville R. S., Kravtsov A. V., Klypin A. A., Primack J. R., Dekel A., 2001, MNRAS, 321, 559
Bussmann R. S. et al., 2008, ApJ, 681, L73
Calura F., Pipino A., Matteucci F., 2008, A&A, 479, 669
Calzetti D., Chandar R., Lee J. C., Elmegreen B. G., Kennicutt R. C., Whitmore B., 2010, ApJ, 719, L158
Cappellari M. et al., 2012, Nat, 484, 485
Ceverino D., Dekel A., Bournaud F., 2010a, MNRAS, 440
Ceverino D., Dekel A., Bournaud F., 2010b, MNRAS, 404, 2151
Choi J.-H., Nagamine K., 2012, MNRAS, 419, 1280
Conroy C., Gunn J. E., 2010, ApJ, 712, 833
Conroy C., van Dokkum P., 2012, ApJ, 747, 69
Conroy C., Gunn J. E., White M., 2009, ApJ, 699, 486
Conroy C., White M., Gunn J. E., 2010, ApJ, 708, 58
Cox T. J. et al., 2006, ApJ, 650, 791
Crosthwaite L. P., Turner J. L., 2007, AJ, 134, 1827
Da Rio N., Robberto M., Hillenbrand L. A., Henning T., Stassun K. G., 2012, ApJ, 748, 14
Daddi E. et al., 2005, ApJ, 631, L13
Daddi E. et al., 2007, ApJ, 670, 156
Daddi E. et al., 2010a, ApJ, 714, L118
Daddi E. et al., 2010b, ApJ, 713, 686
Davé R., 2008, MNRAS, 385, 147
Davé R., 2011, in Treyer M., Wyder T., Neill J., Seibert M., Lee J., eds, ASP Conf. Ser. Vol. 440, UP2010: Have Observations Revealed a Variable Upper End of the Initial Mass Function? Astron. Soc. Pac., San Francisco, p. 353
Davé R., Gardner J., Hernquist L., Katz N., Weinberg D., 2000, in Mazure A., Le Fèvre O., Le Brun V., eds, ASP Conf. Ser. Vol. 200, Clustering at High Redshift, Astron. Soc. Pac., San Francisco, p. 173
Davé R., Finlator K., Oppenheimer B. D., Fardal M., Katz N., Kereš D., Weinberg D. H., 2010, MNRAS, 404, 1355
Davé R., Oppenheimer B. D., Finlator K., 2011, MNRAS, 415, 11
Dekel A. et al., 2009a, Nat, 457, 451
Dekel A. et al., 2009b, Nat, 457, 451
Draine B. T., Li A., 2007, ApJ, 657, 810
Dwek E., 1998, ApJ, 501, 643
Elbaz D. et al., 2007, A&A, 468, 33
Elmegreen B. G., 2002, ApJ, 577, 206
Elmegreen B. G., Klessen R. S., Wilson C. D., 2008, ApJ, 681, 365
Elsner F., Feulner G., Hopp U., 2008, A&A, 477, 503
Engel H. et al., 2010, ApJ, 724, 233
Evans N. J., II, 1999, ARA&A, 37, 311
Evans N. J., II et al., 2009, ApJS, 181, 321
Fakhouri O., Ma C.-P., 2008, MNRAS, 386, 577
Fardal M. A., Katz N., Weinberg D. H., Davé R., 2007, MNRAS, 379, 985
Feldmann R., Gnedin N. Y., Kravtsov A. V., 2011, ApJ, 732, 115
Finlator K., Davé R., Papovich C., Hernquist L., 2006, ApJ, 639, 672
Förster Schreiber N. M., Genzel R., Lutz D., Sternberg A., 2003, ApJ, 599, 193
Fukui Y., Kawamura A., 2010, ARA&A, 48, 547
Fumagalli M., da Silva R. L., Krumholz M. R., 2011, ApJ, 741, L26
Gao Y., Solomon P. M., 2004a, ApJS, 152, 63
Gao Y., Solomon P. M., 2004b, ApJ, 606, 271
Garcia-Burillo S., Usero A., Alonso-Herrero A., Gracia-Carpio J., Pereira-Santaella M., Colina L., Planesas P., Arribas S., 2012, A&A, 539, 8
Gennaro M., Brandner W., Stolte A., Henning T., 2011, MNRAS, 412, 2469
Genzel R. et al., 2010, MNRAS, 407, 2091
Genzel R. et al., 2012, ApJ, 746, 69
Gnedin N. Y., Kravtsov A. V., 2010, ApJ, 714, 287
González V., Labbé I., Bouwens R. J., Illingworth G., Franx M., Kriek M., Brammer G. B., 2010, ApJ, 713, 115
González J. E., Lacey C. G., Baugh C. M., Frenk C. S., 2011, MNRAS, 413, 749
Governato F. et al., 2009, MNRAS, 398, 312
Greve T. R. et al., 2005, MNRAS, 359, 1165
Guo Q., White S. D. M., 2008, MNRAS, 384, 2
Hayward C. C., Narayanan D., Jonsson P., Cox T. J., Kereš D., Hopkins P. F., Hernquist L., 2010, in Treyer, Lee, Seibert, Wyder, Neil eds. Conf. Proc. UP2010: Have Observations Revealed a Variable Upper End of the Initial Mass Function? preprint (arXiv:1008.4584)
Hayward C. C., Kereš D., Jonsson P., Narayanan D., Cox T. J., Hernquist L., 2011, ApJ, 743, 159
Heiderman A., Evans N. J., II, Allen L. E., Huard T., Heyer M., 2010, ApJ, 723, 1019
Hernquist L., 1990, ApJ, 356, 359
Hocuk S., Spaans M., 2010, A&A, 522, A24
Hocuk S., Spaans M., 2011, A&A, 536, A41
Hopkins A. M., Beacom J. F., 2006, ApJ, 651, 142
Hopkins P. F., Younger J. D., Hayward C. C., Narayanan D., Hernquist L., 2010, MNRAS, 402, 1693
Hoversten E. A., Glazebrook K., 2008, ApJ, 675, 163
Iono D. et al., 2009, ApJ, 695, 1537
Johnstone D., Fich M., Mitchell G. F., Moriarty-Schieven G., 2001, ApJ, 559, 307
Jonsson P., 2006, MNRAS, 372, 2
Jonsson P., Primack J. R., 2010, New Astron., 15, 509
Jonsson P., Groves B. A., Cox T. J., 2010, MNRAS, 403, 17
Kang X., Lin W. P., Skibba R., Chen D. N., 2010, ApJ, 713, 1301
Kennicutt R. C., Jr, 1998a, ARA&A, 36, 189
Kennicutt R. C., Jr, 1998b, ApJ, 498, 541
Kennicutt R. C., Jr, Evans N. J., II, 2012, prepint (arXiv:1204.3552)
Kennicutt R. C., Jr et al., 2007, ApJ, 671, 333
Kereš D., Katz N., Weinberg D. H., Davé R., 2005, MNRAS, 363, 2
Kereš D., Katz N., Fardal M., Davé R., Weinberg D. H., 2009, MNRAS, 395, 160
Keres D., Vogelsberger M., Sijacki D., Springel V., Hernquist L., 2011, preprint (arXiv:1109.4638)
Kim S. S., Figer D. F., Kudritzki R. P., Najarro F., 2006, ApJ, 653, L113
Klessen R. S., Spaans M., Jappsen A.-K., 2007, MNRAS, 374, L29
Koda J., Yagi M., Boissier S., Gil de Paz A., Imanishi M., Donovan Meyer J., Madore B. F., Thilker D. A., 2012, ApJ, 749, 20
Kroupa P., 2002, Sci, 295, 82
Krumholz M. R., 2011, ApJ, 743, 110
Krumholz M. R., Dekel A., 2011, preprint (arXiv:1106.0301)
Krumholz M. R., McKee C. F., 2005, ApJ, 630, 250
Krumholz M. R., Tan J. C., 2007, ApJ, 654, 304
Krumholz M. R., Thompson T. A., 2007, ApJ, 669, 289
Krumholz M. R., McKee C. F., Tumlinson J., 2008, ApJ, 689, 865
Krumholz M. R., McKee C. F., Tumlinson J., 2009a, ApJ, 693, 216
Krumholz M. R., McKee C. F., Tumlinson J., 2009b, ApJ, 699, 850
Krumholz M. R., Leroy A. K., McKee C. F., 2011, ApJ, 731, 25
Krumholz M. R., Dekel A., McKee C. F., 2012a, ApJ, 745, 69
Krumholz M. R., Dekel A., McKee C. F., 2012b, ApJ, 745, 69
Lada C. J., Lada E. A., 2003, ARA&A, 41, 57
Lada C. J., Forbrich J., Lombardi M., Alves J. F., 2012, ApJ, 745, 190
Larson R. B., 2005, MNRAS, 359, 211
Lee J. C. et al., 2009, ApJ, 706, 599
Leitherer C. et al., 1999, ApJS, 123, 3
Lemaster M. N., Stone J. M., 2008, ApJ, 682, L97
Leroy A. K. et al., 2011, ApJ, 737, 12
Luhman K. L., 2004, ApJ, 617, 1216
Luhman K. L., Briceño C., Stauffer J. R., Hartmann L., Barrado y Navascués D., Caldwell N., 2003, ApJ, 590, 348
McKee C. F., Ostriker J. P., 1977, ApJ, 218, 148
McKee C. F., Ostriker E. C., 2007, ARA&A, 45, 565
McLure R. J. et al., 2011, MNRAS, 418, 2074

Madau P., Ferguson H. C., Dickinson M. E., Giavalisco M., Steidel C. C., Fruchter A., 1996, MNRAS, 283, 1388
Magnelli B. et al., 2012, A&A, 539, 155
Meurer G. R. et al., 2009, ApJ, 695, 765
Mo H. J., Mao S., White S. D. M., 1998, MNRAS, 295, 319
Motte F., André P., Ward-Thompson D., Bontemps S., 2001, A&A, 372, L41
Narayanan D., Groppi C. E., Kulesa C. A., Walker C. K., 2005, ApJ, 630, 269
Narayanan D., Hayward C. C., Cox T. J., Hernquist L., Jonsson P., Younger J. D., Groves B., 2010, MNRAS, 401, 1613
Narayanan D., Cox T. J., Hayward C. C., Hernquist L., 2011a, MNRAS, 412, 287
Narayanan D., Krumholz M., Ostriker E. C., Hernquist L., 2011b, MNRAS, 418, 664
Narayanan D., Krumholz M. R., Ostriker E. C., Hernquist L., 2012, MNRAS, 421, 3127
Nayakshin S., Sunyaev R., 2005, MNRAS, 364, L23
Niemi S.-M., Somerville R. S., Ferguson H. C., Huang K.-H., Lotz J., Koekemoer A. M., 2012, MNRAS, 421, 1539
Noeske K. G. et al., 2007a, ApJ, 660, L47
Noeske K. G. et al., 2007b, ApJ, 660, L43
Nutter D., Ward-Thompson D., 2007, MNRAS, 374, 1413
Ostriker E. C., Shetty R., 2011, ApJ, 731, 41
Ostriker E. C., Stone J. M., Gammie C. F., 2001, ApJ, 546, 980
Padoan P., Nordlund Å., 2002, ApJ, 576, 870
Papadopoulos P. P., 2010, ApJ, 720, 226
Papadopoulos P. P., Thi W.-F., Miniati F., Viti S., 2011, MNRAS, 414, 1705
Pérez-González P. G. et al., 2008, ApJ, 675, 234
Price D. J., Federrath C., Brunt C. M., 2011, ApJ, 727, L21
Reddy N. A., Steidel C. C., 2009, ApJ, 692, 778
Rieke G. H., Loken K., Rieke M. J., Tamblyn P., 1993, ApJ, 412, 99
Robertson B. E., Kravtsov A. V., 2008, ApJ, 680, 1083
Robertson B., Yoshida N., Springel V., Hernquist L., 2004, ApJ, 606, 32
Robertson B. et al., 2006, ApJ, 641, 21
Rodighiero G. et al., 2011, ApJ, 739, L40
Schruba A. et al., 2011, AJ, 142, 37
Schuster K. F., Kramer C., Hitschfeld M., Garcia-Burillo S., Mookerjea B., 2007, A&A, 461, 143
Shapley A. E., 2011, ARA&A, 49, 525
Shapley A. E., Steidel C. C., Erb D. K., Reddy N. A., Adelberger K. L., Pettini M., Barmby P., Huang J., 2005, ApJ, 626, 698
Shetty R., Ostriker E. C., 2008, ApJ, 684, 978
Shetty R. et al., 2011a, MNRAS, 415, 3253
Shetty R. et al., 2011b, MNRAS, 412, 1686
Silk J., 1997, ApJ, 481, 703
Sobral D., Smail I., Best P. N., Geach J. E., Matsuda Y., Stott J. P., Cirasuolo M., Kurk J., 2012, preprint (arXiv:1202.3436)
Springel V., 2000, MNRAS, 312, 859
Springel V., 2005, MNRAS, 364, 1105
Springel V., Hernquist L., 2003, MNRAS, 339, 289
Springel V., Di Matteo T., Hernquist L., 2005, MNRAS, 361, 776
Stark D. P., Ellis R. S., Bunker A., Bundy K., Targett T., Benson A., Lacy M., 2009, ApJ, 697, 1493
Stolte A., Brandner W., Grebel E. K., Lenzen R., Lagrange A.-M., 2005, ApJ, 628, L113
Tacconi L. J. et al., 2006, ApJ, 640, 228
Tacconi L. J. et al., 2008, ApJ, 680, 246
Tan J. C., 2010, ApJ, 710, L88
Tumlinson J., 2007, ApJ, 664, L63
van Dokkum P. G., 2008, ApJ, 674, 29
van Dokkum P. G., Conroy C., 2011, ApJ, 735, L13
Vázquez G. A., Leitherer C., 2005, ApJ, 621, 695
Vladilo G., 1998, ApJ, 493, 583
Watson D., 2011, A&A, 533, 16
Weingartner J. C., Draine B. T., 2001, ApJ, 548, 296
Weisz D. R. et al., 2012, ApJ, 744, 44
Wilkins S. M., Trentham N., Hopkins A. M., 2008, MNRAS, 385, 687
Wolfire M. G., Hollenbach D., McKee C. F., 2010, ApJ, 716, 1191
Wong T., Blitz L., 2002, ApJ, 569, 157
Wu J., Evans N. J., II, Gao Y., Solomon P. M., Shirley Y. L., Vanden Bout P. A., 2005, ApJ, 635, L173
Wu J., Evans N., Shirley Y., Knez C., 2010, ApJS, 188, 313
Wuyts S. et al., 2011, ApJ, 742, 96

APPENDIX A: A JEANS MASS THAT VARIES WITH THE MEDIAN DENSITY

It is conceivable that one could consider the density term in the Jeans mass equation as the median density (i.e. the density above which half the mass resides), rather than the mean density. As a reminder, while we resolve the surfaces of GMCs, we do not resolve their internal structure. We assume that our GMCs have a lognormal density distribution. In this case, the median density can be expressed in terms of the width of the lognormal, σ_ρ:

$$n_{\rm med} = \bar{n} e^{\sigma_\rho^2/2}, \tag{A1}$$

where $\bar{n}$ is the mean density of the GMC. Numerical experiments suggest that $\sigma_\rho^2 \approx \ln(1 + 3M^2/4)$, where M is the one-dimensional Mach number (Ostriker et al. 2001; Padoan & Nordlund 2002).[8] In Fig. A1, we show the relationship between SFR and $M_{\rm J}$ when the Jeans mass is calculated using $n_{\rm med}$ instead of $\bar{n}$.

The relation between $M_{\rm J}$ and SFR in Fig. A1 is relatively tight. When comparing to Fig. 2, we see that the scatter is greatly reduced when considering a Jeans mass calculated with the $n_{\rm med}$, rather than $\bar{n}$. In Fig. 2, the bulk of the scatter arises from relatively active systems. For example, at a SFR of 50 $M_\odot$ yr^{-1}, the galaxies with the highest average Jeans mass in Fig. 2 are ongoing mergers with warm ISMs, whereas the galaxies with lower Jeans masses are either mergers during a more quiescent phase, or discs. Using the median density rather always results in a Jeans mass that is lower than when using the mean density, due to the extra term that scales with M^2. Because mergers and heavily star-forming discs tend to have high-velocity dispersion gas (e.g. Narayanan et al. 2011b), their Jeans

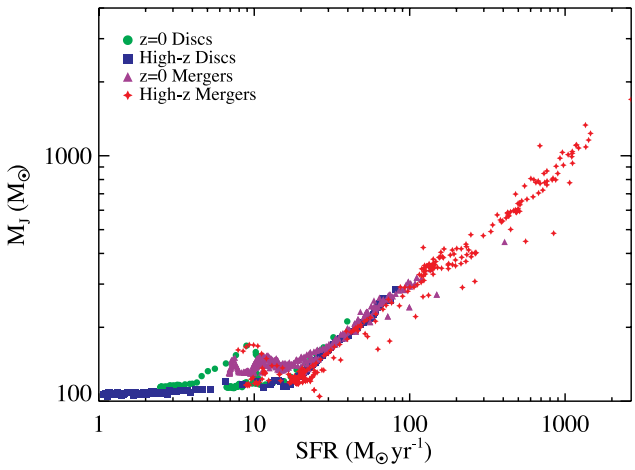

Figure A1. Relationship between SFR and Jeans mass when $M_{\rm J}$ is calculated using the median density in GMCs, rather than the mean. The relation is not dissimilar from using the mean density (see text for details).

[8] We note that other authors have found a range of possible forms for the dependence of σ_ρ [see Lemaster & Stone (2008) and Price, Federrath & Brunt (2011)].

masses are reduced substantially when using $n_{\rm med}$. This tightens the dispersion dramatically in the range SFR = 10–100 $M_\odot\ yr^{-1}$.

One consequence of using $n_{\rm med}$ rather than $\bar{n}$ is that a significant increase in the characteristic mass of the IMF is only seen in heavily star-forming galaxies (SFR $\gtrsim$ 100 $M_\odot\ yr^{-1}$). This suggests that such a variation may only be seen during short-lived phases in local mergers, or in more heavily star-forming galaxies at high redshift.

The results of this paper change little when utilizing $n_{\rm med}$ rather than $\bar{n}$ in the Jeans mass calculation. The normalization of the $M_{\rm J}$–SFR relation in Fig. A1 decreases, while the exponent increases slightly. These effects cause the normalization of equation (4) to decrease by a factor of ∼2, while the exponent decreases to ∼0.85.

This paper has been typeset from a TEX/LATEX file prepared by the author.